Engineering Failure Analysis 146 (2023) 107074

Contents lists available at ScienceDirect

Engineering Failure Analysis

journal homepage: www.elsevier.com/locate/engfailanal

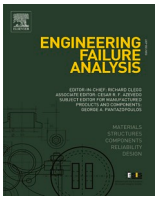

Mechanical performance and failure behavior of screw-bonded joints of aluminum sheets and cross-laminated birch veneer plates

Josef Domitner [a,*], Zahra Silvayeh [a], Jožef Predan [b], Eva Graf [a], Thomas Krenke [c], Nenad Gubeljak [b]

[a] Graz University of Technology, Institute of Materials Science, Joining and Forming, Research Group of Lightweight and Forming Technologies, Inffeldgasse 11/I, 8010 Graz, Austria
[b] University of Maribor, Faculty of Mechanical Engineering, Chair of Mechanics, Smetanova ulica 17, 2000 Maribor, Slovenia
[c] Innovation Centre W.E.I.Z., W.E.I.Z. Forschungs & Entwicklungs gGmbH, Franz-Pichler-Straße 30, 8160 Weiz, Austria

ARTICLE INFO

Keywords:
Lightweight design
Multi-material car body
Aluminum alloy
Wood veneer
Aluminum-wood joints
Hybrid joining
Static strength
Fatigue performance

ABSTRACT

Integrating wood-based lightweight components into advanced multi-material car bodies requires capable and reliable technologies for joining or bonding of dissimilar materials. Therefore, the present experimental study investigates hybrid lap joints of 1.5 mm-thick sheets of EN AW-6016-T4 aluminum alloy and 9 mm- or 13 mm-thick plates of cross-laminated 1 mm-thick birch veneers. Two self-cutting screws and single-component polyurethane-based adhesive were used for each joint. The mechanical performance and the fracture behavior were tested under both quasi-static and cyclic shear-tensile loadings. At each load condition fracture of the joint occurred, but neither fracture of the aluminum alloy sheet nor fracture of the veneer plate were observed. Debonding of the aluminum alloy sheet from the birch veneer plate was identified as critical failure mechanism. The adhesive provided the main contribution to both the static strength and the fatigue performance of the joints. However, the energy absorption of the joint was mainly determined by the pull-out resistance of the screws, which was dependent on the thickness of the veneer plate. To optimize the strength-to-weight ratio of the joint and to exploit the load-bearing potential of the materials, the focus should be placed on the improvement of the bonding conditions or on the adaptation of the sheet/plate thicknesses.

1. Introduction

To reduce the fuel consumption and thus to decrease CO_2 emissions, the automotive industry is shedding the weight of cars wherever possible. Significant weight reduction of car bodies can be achieved by substitution of conventional mild steels with materials of higher strength-to-weight ratio, such as advanced high-strength steels, light metal alloys and composite materials [1,2]. At the beginning of the last century different kinds of wood, in particular hard and soft maple, elm, birch, beech, oak, gum, pine and ash, were extensively used for car body purposes. An early review on "Wood for automobile bodies" published in 1924 proposed that "Wood has held a most important place in the vehicle industry from the earliest times" and that "Its consumption vastly increased with the phenomenal growth of the automobile industry…" [3].

Even though the importance of wood has apparently diminished since then and it has not been in the main focus of car

* Corresponding author.
E-mail address: josef.domitner@tugraz.at (J. Domitner).

https://doi.org/10.1016/j.engfailanal.2023.107074
Received 20 November 2022; Received in revised form 10 January 2023; Accepted 15 January 2023
Available online 20 January 2023

manufacturers until today, it would generally offer great technological, economical and ecological potentials for automotive lightweight applications. Wood and wood-based composites can be used for design and trim components, but also for load-bearing and crash-relevant structural components [4–7]. However, integrating wood into advanced multi-material car bodies is only possible, if capable, reliable and efficient technologies for dissimilar joining with other lightweight materials are available.

A variety of thermal, mechanical, chemical and hybrid technologies for joining of dissimilar materials exist, in particular for use in automotive series production [8]. While resistance spot welding (RSW) has been established as standard technology for thermal joining of steel-based car bodies [9], hybrid technologies which combine mechanical joining by plastic deformation [10–12] with adhesive bonding [13–15] are predominant for producing aluminum-based and multi-material car bodies. Compared to RSW or to simple mechanical joining, hybrid joining improves considerably the load-bearing capacity of structures. For instance, recently performed comprehensive studies on riv-bonding (combines self-piercing riveting and adhesive bonding) revealed that the adhesive layer between the metal sheets influences both the joining process and the joint formation [16], but hybrid riv-bonded joints possess significantly higher static strength, fatigue performance and energy absorption than simple self-piercing-riveted joints [17–20].

Mechanical connections and fastenings [21,22] without the aid of adhesives by various types of traditional carpentry joints [23], nails [24], screws [25], bolts [26,27] or metal plate connectors (MPC) [28] have been common practice in the timber construction industry since decades or even centuries. Mechanical fastening of wood with metals would basically be an option in the automotive industry, and the feasibility of mechanical joining by plastic deformation has already been proven at lab-scale (e.g., flat clinching [29,30] and friction-based processes [31,32] were proposed for spot joining of aluminum alloys with wood). However, as the available design space in car body structures is usually quite limited, the additional use of adhesive may significantly improve the specific load-bearing capacity of the joints. Moreover, efficient joining processes with short cycle times are preferred, which require only single-side access to the components to be joined.

In particular, screw-bonding fulfils these requirements. Hybrid screw-bonded joints possess both the high initial stiffness of the adhesive and the high energy absorption of the screws [33]. Automated setting of the screws can be accomplished within less than a second. However, the liquid adhesive must wet the entire wood surface to achieve reliable bonding. Hydrodynamic flow due to contact pressure and capillary action cause the adhesive to penetrate into the voids of the porous cell structure below the wood surface. Deeper penetration and diffusion into the cell walls increase the effective contact area which improves bonding between adhesive and wood [34–36]. Excellent bonding is generally achieved, if the wood breaks apart from the adhesive joint, which indicates that the strength of the adhesive bond is greater than the strength of the wood.

Simple screwing of plywood and of massive or cross-laminated timber has extensively been studied with focus on different aspects of the pull-out behavior, e.g., in [39–41]. However, great lack of knowledge on hybrid screw-bonding of comparatively thin wood-based materials with light metals exists, especially with regard to the application in lightweight car bodies. Therefore, the present work investigates the load-bearing capacity of hybrid screw-bonded joints of commercial EN AW-6016-T4 aluminum alloy sheets and of cross-laminated birch veneer plates under both quasi-static and cyclic loadings. Based on the detailed assessment of the mechanical performance and the fracture behavior, measures for optimizing the hybrid joints are proposed.

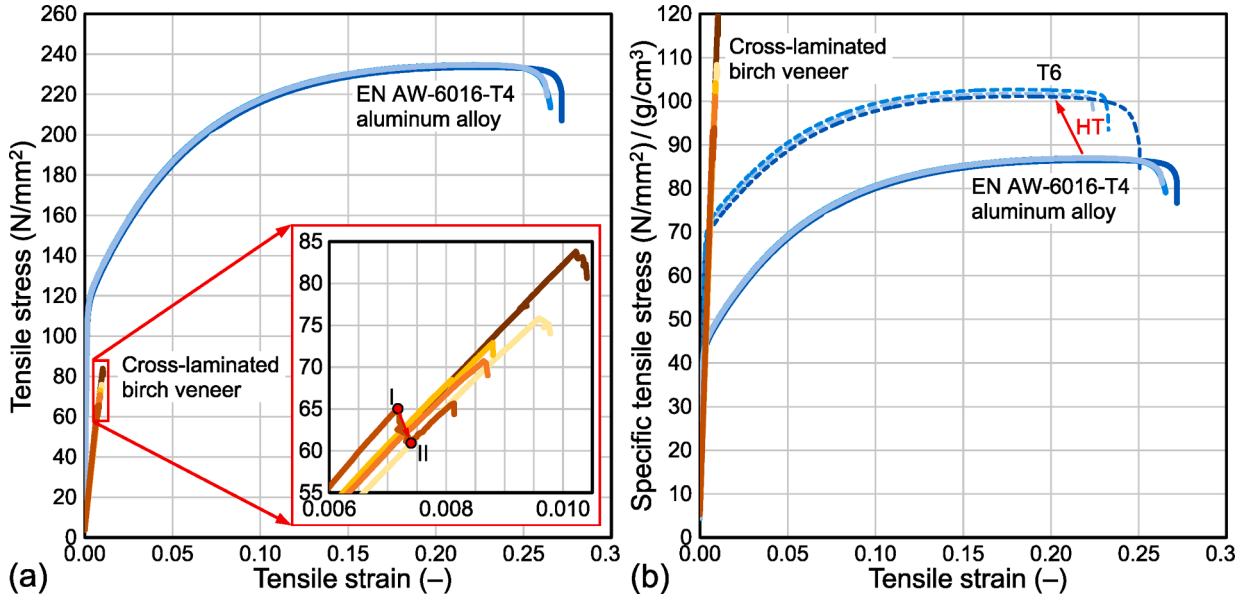

Fig. 1. Comparison of (a) technical tensile stress–strain curves and (b) tensile stress–strain curves of the EN AW-6016-T4 aluminum alloy and of the cross-laminated birch veneers normalized by the density. The discontinuity of the stress–strain curve (I → II) was due to the abrupt failure of the veneer at the surface of the sample.

2. Materials and methods

2.1. Material specifications

Sheets with dimensions of 100 mm × 90 mm were shear-cut by using a hydraulic guillotine from commercial 1.5 mm-thick EN AW-6016-T4 aluminum alloy which is typically used for producing outer panels of car bodies. The edges of the sheets were maintained as-cut, as the edge condition of the aluminum alloy sheets was classified as uncritical under both quasi-static (monotonic-static) and cyclic (cyclic-dynamic) loads [37]. Plates with dimensions of 100 mm × 90 mm were cut by using a disk saw from 9 mm- or 13 mm-thick panels consisting of 1 mm-thick cross-laminated birch veneers. The densities of the aluminum alloy sheet and of the laminated birch veneer plate with the moisture content of about 4–5 wt% were 2.7 g/cm^3 and about 0.7 g/cm^3, respectively.

Fig. 1(a) compares the stress–strain curves obtained from tensile testing of both the aluminum alloy sheets in rolling direction and the cross-laminated birch veneers plates. Bone-shaped samples with dimensions according to DIN 50125 were prepared for tensile testing. Young's modulus, ultimate tensile strength and strain to fracture of the aluminum alloy and of the cross-laminated veneers were about 71×10^3 N/mm^2 and 8.1×10^3 N/mm^2, 234 N/mm^2 and 74 N/mm^2, as well as 26.8 % and 0.1 %, respectively. It is evident that the birch veneers did not possess any notable ductility. The tensile properties of the three aluminum alloy samples were almost identical, but the ultimate tensile strength determined from five cross-laminated birch veneer samples showed considerable scatter of about ± 10 N/mm^2. Initiation of fracture was identical for each of these samples: firstly the veneer located at the surface of the sample and oriented perpendicular to the loading direction failed. The detail of Fig. 1(a) illustrates, that abrupt initial failure of the veneer at the surface may cause a discontinuity (I → II) in the stress–strain curve.

The strength of the cross-laminated birch veneers was only about $^1/_3$ of the strength of the aluminum alloy in condition T4. However, as shown in Fig. 1(b), the specific strengths (i.e., the strength normalized by the density of the material) of the laminated veneers and of the aluminum alloy in peak-aged condition T6 were very similar. For both materials the mean specific strength was about 100 (N/mm^2)/(g/cm^3), that is 10^5 Nm/kg. Condition T6 can be achieved by heat treatment (HT) of the aluminum alloy in naturally-aged condition T4, e.g., at about 180–200 °C for 20 min as described elsewhere [19,20]. However, to avoid irreversible thermal degradation of lignin above 150 °C [38], the aluminum alloy should be heat-treated before dissimilar joining.

2.2. Screw-bonding process

The aluminum alloy sheets were screw-bonded with the veneer plates using two standard ST4.8×16 bright zinc-plated (BZP) steel pan head drilling screws according to ISO 15481 with tapping screw thread and drill tip, as well as about 0.25 g (140 g/m^2) of commercial liquid Collano RP 2760 single-component polyurethane-(PUR)-based adhesive [42]. This adhesive had also been used for gluing the veneers. PUR-based adhesives possess the lowest elastic modulus and thus the highest flexibility among the relevant wood adhesives [43], which has been supposed as beneficial for the present application.

Additional treatments would complicate the joining process and thus increase the overall process costs in series production; therefore, the aluminum alloy sheet was used in as-received condition. Only pilot holes for the screws with the diameter of 5 mm were drilled. Before the liquid adhesive was homogeneously distributed on the total bonding area of 90 mm × 20 mm, each sheet had been cleaned firstly with nitro dilution and secondly with ethanol. After applying the adhesive, the aluminum alloy sheet and the laminated veneer plate were put together and the screws were driven into the veneer plate using a cordless screwdriver. The required torque for tightening the screws depends mainly on the thickness of the veneer plate [44]. By using a torque wrench the screws were finally tightened with the defined torques of 2 Nm and 4 Nm for samples consisting of 9 mm-thick and 13 mm-thick plates, respectively.

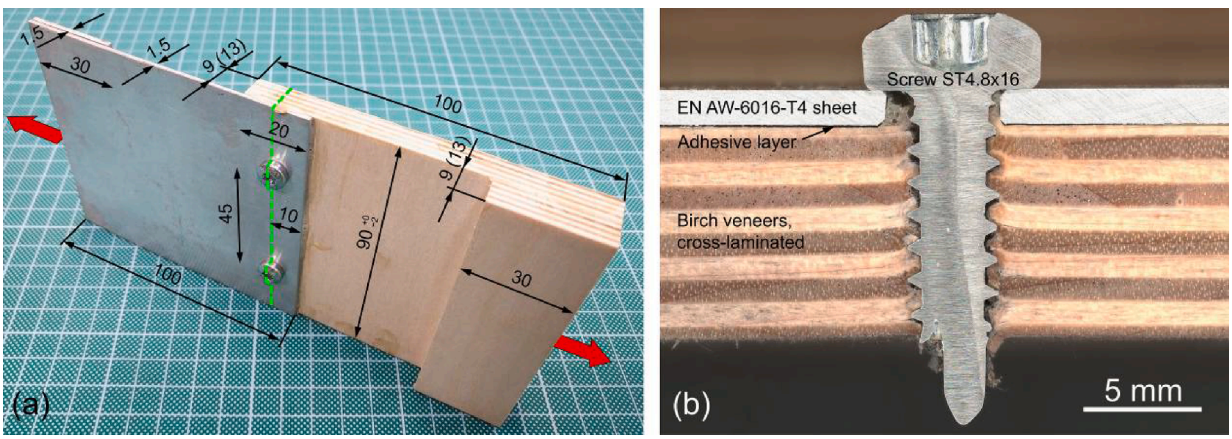

Fig. 2. (a) Dimensions of screw-bonded aluminum-wood sample. The red arrows indicate the loading direction and the green dashed line marks the position where the sample was sectioned. (b) Detailed view on the cross-section of the joint showing veneer fibers which are oriented parallel (dark brown) and perpendicular (light brown) to the view direction.

Tightening the screws distributed the adhesive between the sheet and the plate, and portions of the adhesive were even squeezed out of the joining gap.

As illustrated in Fig. 2(a), total length, total width and overlapping length of the screw-bonded samples were approx. 180 mm, 90 mm and 20 mm, respectively. The distance between the screws was 45 mm. Using identical sample dimensions as in previous studies [19,20] enabled comparing the load-bearing capacities of aluminum-wood joints with load capacities of typical self-piercing-riveted and riv-bonded Al-Al and Al-Mg lap joints. To ensure that the tensile load was applied in-plane with the adhesive layer, a 1.5 mm-thick spacing strip was glued onto the backside of the aluminum alloy sheet, and a 9 mm- or 13 mm-thick spacing plate was glued onto the backside of the veneer plate. The dimensions of the spacing strip and plate were 90 mm × 30 mm.

To evaluate the joint integrity a representative sample was sectioned directly at the joint as marked with the green dashed line in Fig. 2(a). Fig. 2(b) provides a detailed view on the cross-section of this joint. The layered structure of the veneer plate and the fibre orientation of the veneers is quite well visible. It is evident that the adhesive layer between the upper aluminum alloy sheet and the lower veneer plate was thin (< 0.1 mm) and uniform. Hence, a homogeneous distribution of the adhesive was achieved in the applied joining process. Moreover, closer examination of the cross-section reveals localized deformation of the veneers and even initiation of first microcracks next to the thread of the screw. Any further increase of the torque for tightening the screws would therefore enhance local damage of the veneers at the surface of the screw hole.

2.3. Testing procedure

To ensure comparability of the results, the procedure for testing the aluminum-wood joints was based on the procedure proposed for testing of Al-Al [19] and Al-Mg [20] joints. Therefore, a spindle-driven Zwick/Roell Z100 testing machine was used for quasi-static testing, whereas a servo-hydraulic Instron 1255 testing machine was used for cyclic testing. The testing speed for determining the quasi-static load maximum was 5 mm/min. Sinusoidal cyclic loading with the load ratio of $R = 0.1$ (ratio between the cyclic load minimum, F_{min}, and the cyclic load maximum, F_{max}) was applied with frequencies between 3 Hz at the low-cycle fatigue regime and 8 Hz at the high-cycle fatigue regime. $R > 0$ indicates that the samples were always exposed to tension during cyclic testing. If the sample did not fail although about 2 million cycles had been reached, cyclic testing was stopped. The highest load amplitude which did not cause fracture/failure was considered as fatigue limit. After testing the fracture surfaces were captured using a Keyence VHX-7100 digital microscope equipped with a VHX-E20 objective lens for high-resolution three-dimensional imaging.

3. Results and discussion

3.1. Static properties

Fig. 3(a) shows the tensile force–displacement curves monitored during quasi-static shear-tensile testing of samples with 9 mm-thick (green lines) and 13 mm-thick (blue lines) cross-laminated birch veneer plates. The tensile force increased almost linearly to the maximum of about 12 kN. Once brittle failure of the adhesive layer between the aluminum alloy sheet and the veneer plate occurred at the displacement of 2–3 mm, the tensile force abruptly decreased to 2–3 kN. This characteristic behavior was observed for each of the six samples tested. Hence, the static strength (i.e., the maximum tensile force) of the hybrid joints was dependent on the load-bearing

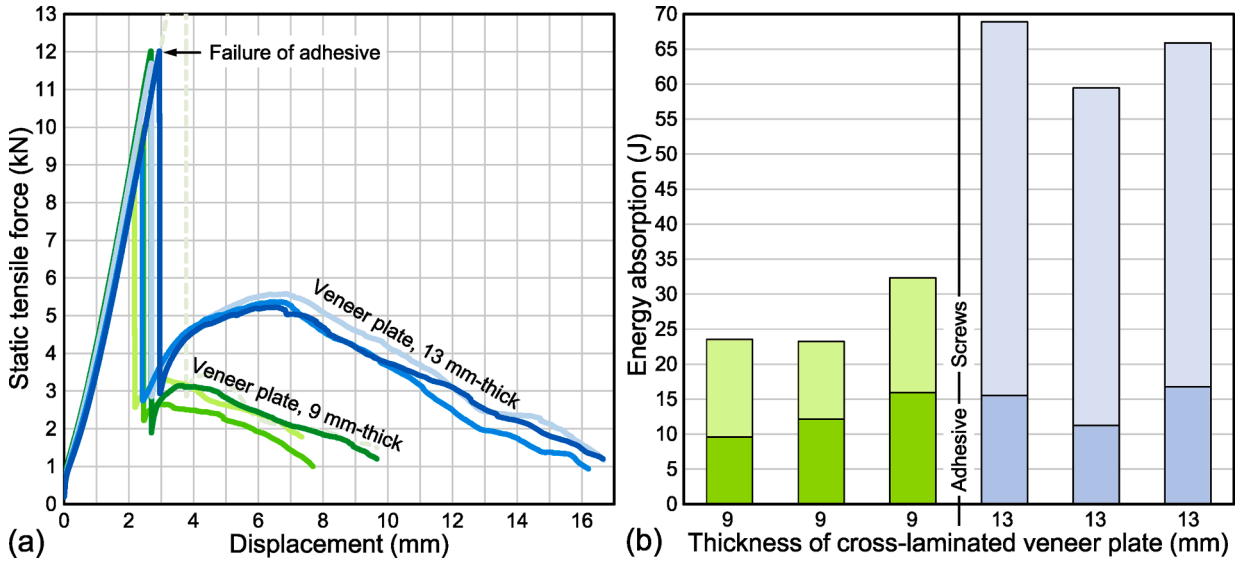

Fig. 3. Comparison of (a) force–displacement curves and (b) energy absorption in quasi-static testing of screw-bonded lap joints of 1.5 mm-thick aluminum alloy sheets and 9 mm-thick or 13 mm-thick cross-laminated birch veneer plates.

capacity of the adhesive layer between the aluminum alloy sheet and the cross-laminated veneer plate, but it was actually independent from the thickness of the veneer plate.

However, Fig. 3(a) also illustrates that the force–displacement curves and thus the fracture behavior of the hybrid joints were considerably influenced by the thickness of the cross-laminated birch veneer plates for displacements beyond 3 mm. The tensile force increased notably to about 5.1–5.6 kN at the displacement of 6–7 mm for samples consisting of 13 mm-thick veneer plates (blue lines), but just a negligible increase of the tensile force was monitored for samples consisting of 9 mm-thick veneer plates (green lines). This difference is related to the pull-out resistance of the screws, which generally increases with growing number of the veneers and with increasing thickness of the cross-laminated veneer plate. Hence, the screws do not influence the strength, but the energy absorption of the joints under quasi-static loading. This characteristic fracture behavior of hybrid screw-bonded metal-wood lap joints, which includes the high initial stiffness of the adhesive and the high energy absorption of the screws, was recently confirmed [33].

The energy absorption of each joint was calculated by numerical integration of the area below each of the force–displacement curves shown in Fig. 3(a). The absorption of the adhesive was calculated from zero displacement to the displacement at maximum force, i.e., when failure of the adhesive layer occurred, whereas the absorption of both screws was calculated from the displacement at maximum force to the maximum displacement, i.e., when the shear-tensile test was stopped. Fig. 3(b) illustrates that the energy absorbed particularly by the adhesive was quite similar for each of the six joints. It was in the range of 10–17 J, which is about half of the total energy absorbed by the joints with the 9 mm-thick veneer plate (green bars), but less than a quarter of the total energy absorbed by the joints with the 13 mm-thick veneer plate (blue bars). Hence, increasing the thickness of the cross-laminated veneer plate from 9 mm to 13 mm more than doubled the total energy absorption capacity of the joints to about 60–70 J. In order to characterize the performance of screw-bonded joints under crash loadings experimental verification of these results at high testing speeds would be mandatory.

3.2. Fatigue performance

As the static strength of the joints was independent from the thickness of the cross-laminated veneer plate, only samples consisting of 1.5 mm-thick aluminum alloy sheets and of 9 mm-thick plates were used for cyclic testing. Fig. 4 correlates the load amplitude applied during cyclic testing, F_{amp}, with the number of cycles, N, counted until fracture of the joints occurred. In general, N tends to increase with decreasing F_{amp}. The markers with arrows represent samples which did not fail at 2 million cycles. Fracture occurred exclusively at the adhesive layer between the aluminum alloy sheet and the veneer plate. After the adhesive had failed, the screws were immediately pulled out of the veneer plate, as observed in quasi-static testing. This basic fracture behavior of the screw-bonded joints was identical at each of the load amplitudes tested.

The scatter of the green circular markers in Fig. 4 is much larger than the scatter of the square markers representing conventional self-piercing-riveted lap joints of 1.5 mm-thick aluminum alloy sheets [19]. Within the low-cycle fatigue regime at $F_{amp} = 2.7$ kN self-piercing-riveted aluminum joints possess about ten-times greater N than screw-bonded aluminum-birch joints. With decreasing load amplitude this difference becomes smaller, and at low $F_{amp} \approx 1.5$ kN (i.e., within the high-cycle fatigue regime) the difference is negligible. Nevertheless, the fatigue performance of screw-bonded joints of aluminum sheets and birch veneer plates does not reach the performance of riv-bonded joints of metal sheets [19,20] that are state-of-the-art in manufacturing of lightweight car bodies.

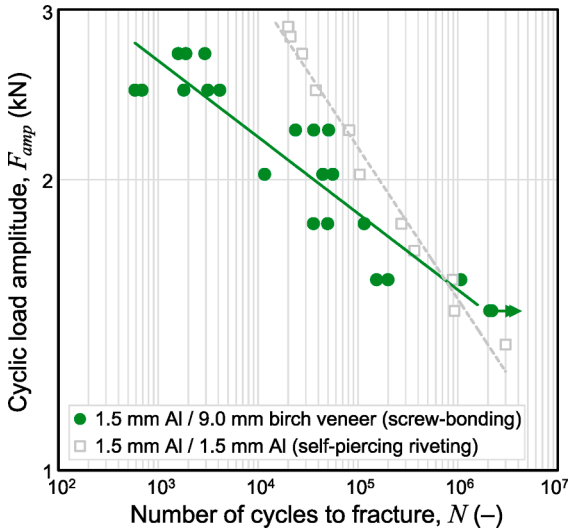

Fig. 4. Fatigue curves of screw-bonded lap joints of 1.5 mm-thick aluminum alloy sheets and 9 mm-thick cross-laminated birch veneer plates, and of self-piercing-riveted lap joints of 1.5 mm-thick aluminum alloy sheets [19]. Both joint types were tested at the load ratio of $R = 0.1$ using samples with identical basic dimensions.

3.3. Failure analysis

Fig. 5(a) shows the typical fracture behavior of screw-bonded aluminum-wood joints under shear-tensile load as observed in this work. In quasi-static as well as in cyclic testing the screws were immediately pulled out of the veneer plate, after the aluminum alloy sheet and the veneer plate had debonded and separated from each other. A combination of three basic failure mechanisms as schematically illustrated in Fig. 5(b) was observed: (i) adhesive failure between the adhesive layer and the aluminum alloy sheet or the veneer plate, (ii) cohesive failure of the adhesive layer, and (iii) cohesive failure of the veneer plate.

The three failure mechanisms did not occur together at each of the joints. In cyclic testing the cohesion-based mechanisms (ii) and (iii) were only occasionally observed, whereas the adhesion-based mechanism (i) was by far dominant when using the PUR-based adhesive for gluing aluminum with wood. This trend was independent from the applied load amplitude F_{amp}. Hence, any clear relationship between a particular failure mechanism and F_{amp} as proposed, e.g., for riv-bonded Al-Al [19] and Al-Mg [20] lap joints was not observed. However, comparing the fatigue performance of the joints at constant F_{amp} revealed that N tended to increase when the cohesion-based failure mechanism (iii) became more apparent.

The quite erratic failure behavior of the adhesive bonding under cyclic loading was the main reason for the varying fatigue performance, as indicated by large scatter of the markers in Fig. 4. Nevertheless, under static loading the behavior of the joints was very similar, as indicated by the overlapping curves in Fig. 3. Hence, the PUR-based adhesive used in the present work seems to be critical particularly under cyclic loading.

Fig. 6 compares two joints that failed at comparatively (a) low and (b) high number of cycles at almost identical load amplitude of $F_{amp} \approx 2.2$ kN. The surface of the aluminum alloy sheet in Fig. 6(a) is free from any splinters of wood, and residues of adhesive are only visible on a few percent of the total bonding area. Hence, the adhesion on the aluminum alloy sheet was obviously insufficient. Moreover, the veneer contains a branch structure (brown patch next to the left screw hole), which hindered penetration of the adhesive from the surface of the veneer plate into the wood cells. This may also affect the adhesion on the veneer plate. In contrast, splinters and fragments of wood as well as residues of adhesive are visible on the surface of the sheet in Fig. 6(b). That indicates better adhesion on the surface of the aluminum alloy sheet, although residues of adhesive and wood are only visible on about ¼ of the total bonding area.

As insufficient bonding between the adhesive and the aluminum alloy sheet and/or the veneer plate may reduce the number of cycles to fracture of the joint tremendously, optimization of adhesive bonding is required to improve the fatigue performance. For example, this may be achieved by using adhesives with different properties [43] or by pre-treating the bonding surfaces [45,46].

4. Conclusions

The present experimental study investigates the load-bearing capacity of hybrid screw-bonded lap joints of 1.5 mm-thick EN AW-6016-T4 aluminum alloy sheets and of 9 mm-thick or 13 mm-thick cross-laminated birch veneer plates under shear-tensile loading. Static properties (strength and energy absorption), fatigue performance and fracture behavior of the joints were characterized. The following conclusions were drawn:

(1) At each load condition the joint was critical with regard to the mechanical performance; neither fracture of the aluminum alloy sheet nor fracture of the birch veneer plate occurred. Static strength and fatigue performance of the hybrid joints were mainly

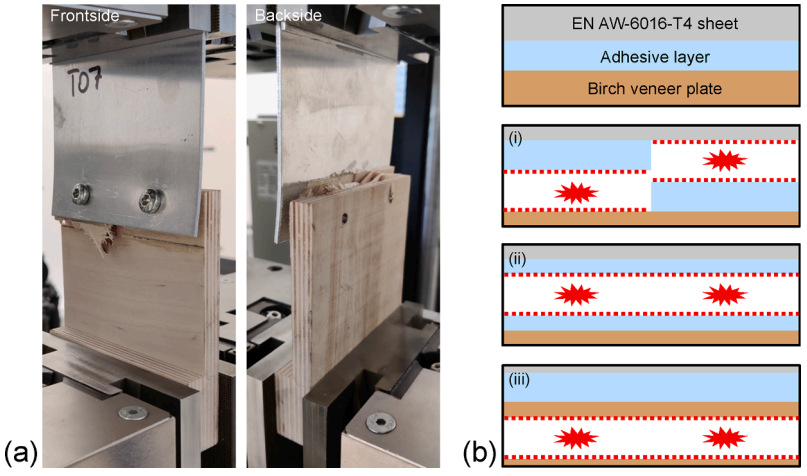

Fig. 5. (a) Typical fracture of screw-bonded lap joints of 1.5 mm-thick aluminum alloy sheet and 9 mm-thick cross-laminated birch veneer plate under shear-tensile loading, and (b) schematic illustration of three basic failure mechanisms: (i) adhesive failure between the adhesive layer and the aluminum alloy sheet or the veneer plate, (ii) cohesive failure of the adhesive layer, and (iii) cohesive failure of the veneer plate. The dashed lines and the jagged symbols indicate the potential locations of failure when the aluminum/adhesive/veneer stack is loaded.

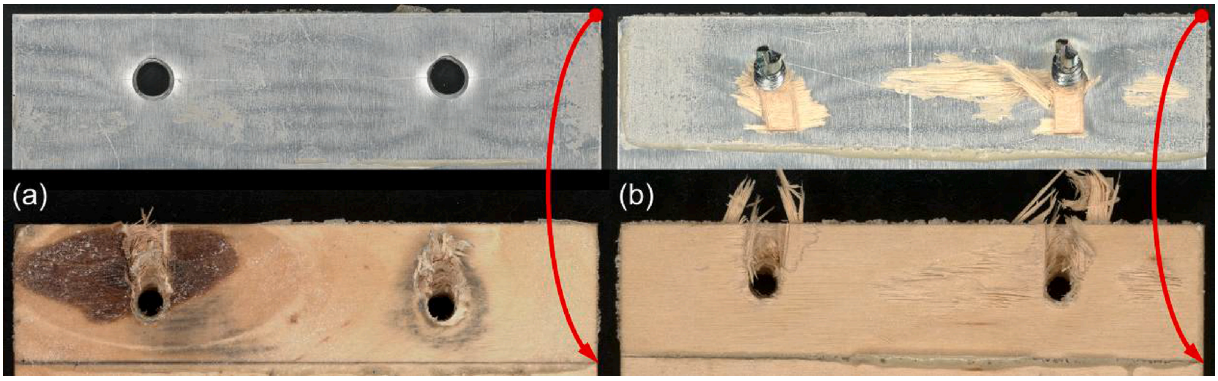

Fig. 6. Comparison of fracture surfaces for (a) insufficient bonding and (b) improved bonding. Both joints were tested at the load ratio of $R = 0.1$ and at the load amplitude of $F_{amp} \approx 2.2$ kN.

dependent on the adhesive bonding between the aluminum alloy sheet and the veneer plate, whereas the screws contributed only little. Debonding was identified as critical failure mechanism.

(2) The static strength of the joints was independent from the thickness of the veneer plate. However, the energy absorption of the joints under quasi-static loading increased notably, if the thickness and thus the pull-out resistance of the screws increased. The screws provided the main contribution to the total energy absorption of the joints, in particular, when the 13 mm-thick veneer plate was used.

(3) To optimize the strength-to-weight ratio, (i) adhesive bonding would need improvement to exploit the load-bearing potentials of the aluminum alloy sheet and of the veneer plate, or (ii) the thicknesses of the sheet and of the plate should be reduced to match the actual load-bearing capacity of the hybrid joint. However, decreasing the plate thickness would impair the energy absorption of the joint.

(4) Further experimental verification of the joint properties at high testing speeds would be required to characterize the crash performance of screw-bonded joints. In particular, the performance of the adhesive at high strain rates must be considered.

Declaration of Competing Interest

The authors declare that they have no known competing financial interests or personal relationships that could have appeared to influence the work reported in this paper.

Data availability

Data will be made available on request.

Acknowledgement

The present study was co-funded by the Scientific & Technological Cooperation program of the Austrian Federal Ministry of Education, Science and Research (BMBWF) and of the Slovenian Ministry for Education, Science and Sport (MESS). This joint program is managed by the Austrian Agency for Education and Internationalization (OeAD) and by the Slovenian Research Agency (ARRS). Samples were prepared within the “Modelling, Production and Further Processing of Eco-Hybrid Structures and Materials” (CARpenTiER) project funded by the Austrian Federal Ministries of Climate Action, Environment, Energy, Mobility, Innovation and Technology (BMK) and of Labor and Economy (BMAW), by the Province of Styria, and by partner companies within the Competence Centers for Excellent Technologies (COMET) program, which is processed by the Austrian Research Promotion Agency (FFG) and by the Styrian Business Promotion Agency (SFG). Open access funding was provided by Graz University of Technology. Thanks to Peter Auer and Luka Ferlič for supporting the shear-tensile tests.

References

[1] A.I. Taub, A.A. Luo, Advanced lightweight materials and manufacturing processes for automotive applications, MRS Bull. 40 (12) (2015) 1045–1053.
[2] A. Taub, E. De Moor, A. Luo, D.K. Matlock, J.G. Speer, U. Vaidya, Materials for Automotive Lightweighting, Annu. Rev. Mat. Res. 49 (2019) 327–359.
[3] A.T. Upson, L.N. Ericksen, Wood for automobile bodies, SAE Trans. 19 (1924) 513–531.
[4] D. Kohl, P. Link, S. Böhm, Wood As A Technical Material For Structural Vehicle Components, Procedia CIRP 40 (2016) 557–561.
[5] G. Baumann, A. Stadlmann, C. Kurzböck, F. Feist, Crash-proof Wood Composites in Lightweight Bodyworks of the Future, ATZ Worldwide 121 (11) (2019) 48–51.
[6] G. Baumann, R. Brandner, U. Müller, C. Kumpenza, A. Stadlmann, F. Feist, Temperature-Related Properties of Solid Birch Wood under Quasi-Static and Dynamic Bending, Materials 13 (2020) 5518.
[7] U. Müller, T. Jost, C. Kurzböck, A. Stadlmann, W. Wagner, S. Kirschbichler, G. Baumann, M. Pramreiter, F. Feist, Crash simulation of wood and composite wood for future automotive engineering, Wood Mat. Sci. Eng. 15 (5) (2020) 312–324.

[8] K. Martinsen, S.J. Hu, B.E. Carlson, Joining of dissimilar materials, CIRP Ann. Manuf. Technol. 64 (2015) 679–699.
[9] M. Pouranvari, S.P.H. Marashi, Critical review of automotive steels spot welding: process, structure and properties, Sci. Technol. Weld. Join. 18 (5) (2013) 361–403.
[10] P. Groche, S. Wohletz, M. Brenneis, C. Pabst, F. Resch, Joining by forming – A review on joint mechanisms, applications and future trends, J. Mater. Process. Technol. 214 (2014) 1972–1994.
[11] K.-I. Mori, Y. Abe, A review on mechanical joining of aluminium and high strength steel sheets by plastic deformation, Int. J. Lightweight Mater. Manuf. 1 (2018) 1–11.
[12] G. Meschut, M. Merklein, A. Brosius, D. Drummer, L. Fratini, U. Füssel, M. Gude, W. Homberg, P.A.F. Martins, M. Bobbert, M. Lechner, R. Kupfer, B. Gröger, D. Han, J. Kalich, F. Kappe, T. Kleffel, D. Köhler, C.-M. Kuball, J. Popp, D. Römisch, J. Troschitz, C. Wischer, S. Wituschek, M. Wolf, Review on mechanical joining by plastic deformation, J. Adv. Join Process 5 (2022) 100113.
[13] S. Budhe, M.D. Banea, S. de Barros, L.F.M. da Silva, An updated review of adhesively bonded joints in composite materials, Int. J. Adhes. Adhes. 72 (2017) 30–42.
[14] F. Cavezza, M. Boehm, H. Terryn, T. Hauffman, A Review on Adhesively Bonded Aluminium Joints in the Automotive Industry, Metals 10 (2020) 730.
[15] S. Maggiore, M.D. Banea, P. Stagnaro, G. Luciano, A Review of Structural Adhesive Joints in Hybrid Joining Processes, Polymers 13 (2021) 3961.
[16] J. Domitner, P. Auer, J. Stippich, Z. Silvayeh, S. Jessernig, L. Peiser, F. Hönsch, C. Sommitsch, Riv-bonding of aluminum alloys with high-strength steels against the favorable joining direction, J. Mater. Eng. Perform. 31 (9) (2022) 6970–6979.
[17] F. Moroni, A. Pirondi, F. Kleiner, Experimental analysis and comparison of the strength of simple and hybrid structural joints, Int. J. Adhes. Adhes. 30 (2010) 367–379.
[18] F. Moroni, Fatigue behaviour of hybrid clinch-bonded and self-piercing rivet bonded joints, J. Adhes. 95 (5–7) (2019) 577–594.
[19] J. Domitner, Z. Silvayeh, J. Predan, P. Auer, J. Stippich, C. Sommitsch, N. Gubeljak, Load-bearing capacities and fracture modes of self-piercing-riveted, adhesive-bonded and riv-bonded aluminum joints at quasi-static and cyclic loadings, J. Mater. Eng. Perform. (2022), https://doi.org/10.1007/s11665-022-07677-5.
[20] J. Domitner, Z. Silvayeh, J. Predan, P. Auer, J. Stippich, N. Enzinger, N. Gubeljak, Load-bearing capacity of hybrid riv-bonded aluminum-magnesium joints at quasi-static and cyclic loadings, J. Manuf. Process. 87 (2023) 133–140.
[21] L.A. Soltis (Ed.), Mechanical Connections in Wood Structures. ASCE Manuals and Reports on Engineering Practice, No. 84, American Society of Civil Engineers (ASCE), New York (NY), 1996.
[22] D.R. Rammer, Fastenings, in: Wood Handbook – Wood as an Engineering Material. General Technical Report FPL–GTR–282. Madison (WI): Forest Products Laboratory, US Department of Agriculture (USDA); 2021.
[23] J.A. Sobon, Historic American Timber Joinery: A Graphic Guide, 2nd ed., Timber Framers Guild, Becket (MA), 2004.
[24] H. Korte, G. Koch, K.C. Krause, Wood nails to fix softwoods: characterization of structural deformation and lignin modification, Eur. J. Wood Wood Prod. 76 (2018) 979–988.
[25] M. Sydor, Geometry of wood screws: a patent review, Eur. J. Wood Wood Prod. 77 (2019) 93–103.
[26] G.W. Trayer, The Bearing Strength of Wood under Bolts. Technical Bulletin 332. Madison (WI): Forest Products Laboratory, US Department of Agriculture (USDA); 1932.
[27] P.J. Moss, Multiple-Bolted Joints in Wood Members – A Literature Review. General Technical Report FPL–GTR–97. Madison (WI): Forest Products Laboratory, US Department of Agriculture (USDA); 1997.
[28] T. Ling, S. Mohrmann, H. Li, N. Bao, M. Gaff, R. Lorenzo, Review on research progress of metal-plate-connected wood joints, J. Build. Eng. 59 (2022) 105056.
[29] S. Lüder, S. Härtel, C. Binotsch, B. Awiszus, Influence of the moisture content on flat-clinch connection of wood materials and aluminum, J. Mater. Process. Technol. 214 (2014) 2069–2074.
[30] T. Gerstmann, B. Awiszus, Hybrid joining: Numerical process development of flat-clinch-bonding, J. Mater. Process. Technol. 277 (2020) 116421.
[31] Y. Xie, Y. Huang, X. Meng, J. Li, J. Cao, Friction stir spot welding of aluminum and wood with polymer intermediate layers, Constr. Build. Mater. 240 (2020), 117952.
[32] Y. Xie, Y. Huang, X. Meng, F. Wang, L. Wan, Z. Dong, J. Cao, Friction rivet joining towards high-performance wood-metal hybrid structures, Compos. Struct. 247 (2020) 112472.
[33] K. Imakawa, Y. Ochiai, K. Aoki, N. Hori, A. Takemura, T. Yamaguchi, Mechanical properties of hybrid joints in timber structures, J. Wood Sci. 68 (2022) 37.
[34] C.R. Frihart, C.G. Hunt, Wood Adhesives – Bond Formation and Performance, in: Wood Handbook – Wood as an Engineering Material. General Technical Report FPL–GTR–282. Madison (WI): Forest Products Laboratory, US Department of Agriculture Forest Service (USDA); 2021.
[35] F.A. Kamke, J.N. Lee, Adhesive penetration in wood – a review, Wood Fiber Sci. 39 (2) (2007) 205–220.
[36] C.G. Hunt, C.R. Frihart, M. Dunky, A. Rohumaa, Understanding Wood Bonds – Going Beyond What Meets the Eye: A Critical Review, Rev. Adhes. Adhes. 6 (4) (2018) 369–440.
[37] J. Domitner, Z. Silvayeh, J. Predan, F. Jerenec, P. Auer, J. Stippich, L. Ferlič, P. Štefane, C. Sommitsch, N. Gubeljak, Influence of the sheet edge condition on the fracture behavior of riv-bonded aluminum-magnesium joints, Key Eng. Mater. 926 (2022) 1541–1548.
[38] C. Hill, M. Altgen, L. Rautkari, Thermal modification of wood – a review: chemical changes and hygroscopicity, J. Mater. Sci. 56 (2021) 6581–6614.
[39] S.-J. Pang, K.-S. Ahn, S.G. Kang, J.-K. Oh, Prediction of withdrawal resistance for a screw in hybrid cross-laminated timber, J. Wood Sci. 66 (2020) 79.
[40] K. Hoelz, P. Grauberger, S. Matthiesen, Investigation of Failure Behavior in the Thread Contact of Wood Screws during the Pull-Out Process, J. Struct. Eng. 146 (10) (2020) 04020211.
[41] K. Hoelz, L. Kleinhans, S. Matthiesen, Wood screw design: influence of thread parameters on the withdrawal capacity, Eur. J. Wood Wood Prod. 79 (2021) 773–784.
[42] A.G. Collano, Data Sheet Collano RP 2760–1C PUR adhesive, Sempach, Switzerland, 2022.
[43] F. Stoeckel, J. Konnerth, W. Gindl-Altmutter, Mechanical properties of adhesives for bonding wood – A review, Int. J. Adhes. Adhes. 45 (2013) 32–41.
[44] C. Kumpenza, G.-D. Schmidt, A. Sotayo, A. Ringhofer, U. Müller, Study on torque and clamping forces of screw-connected plywood, Eng. Rep. 2 (2020) e12211.
[45] G.W. Critchlow, D.M. Brewis, Review of surface pretreatments for aluminium alloys, Int. J. Adhes. Adhes. 16 (1996) 255–275.
[46] J. Žigon, J. Kovač, R. Zaplotnik, J. Saražin, M. Šernek, M. Petrič, S. Dahle, Enhancement of strength of adhesive bond between wood and metal using atmospheric plasma treatment, Cellul. 27 (2020) 6411–6424.